

HETEROCYCLES, Vol. 106, No. 11, 2023, pp. 1866 - 1876. © 2023 The Japan Institute of Heterocyclic Chemistry
Received, 14th September, 2023, Accepted, 13th October, 2023, Published online, 17th October, 2023
DOI: 10.3987/COM-23-14905

**TRIAZENE-BRIDGED NITROGEN-RICH HETEROCYCLIC
ENERGETIC COMPOUNDS 4,4'-(TRIAZ-1-ENE-1,3-DIYL)BIS(1,2,5-
OXADIAZOL-3-AMINE) - SYNTHESIS, CHARACTERIZATION AND
PROPERTIES**

**Jin Zhu, Qianxiong Chen, Suming Jing,* Keyao Li, Zhineng Wang,
Yuanyuan Wang, and Jiahao Deng**

Jin Zhu, Lead-Author, Department of Environmental and Safety Engineering,
North University of China, Taiyuan, Shanxi, China. zhujinzbdx@foxmail.com.

*Su-ming Jing, Corresponding author, Department of Environmental and Safety
Engineering, North University of China, Taiyuan, Shanxi, China.
j782855067@163.com

Abstract – 4,4'-(Triaz-1-ene-1,3-diyl)bis(1,2,5-oxadiazol-3-amine) was designed and synthesized with 3,4-diaminofurazan and triazene bridges, which was fully characterized by NMR, IR, elemental analyses, and single crystal X-ray diffraction. The results of structural and physicochemical characterization of 4,4'-(triaz-1-ene-1,3-diyl)bis(1,2,5-oxadiazol-3-amine) showed that this compound exhibits particularly high formation heats ($\Delta H_f=926.32$ kJ mol⁻¹) which is higher than that of all currently reported furazan-based energetic compounds, excellent detonation performance ($D=8151$ m s⁻¹, $P=28.55$ GPa). In addition, this compound is insensitive to external mechanical stimuli ($IS=40$ J FS=289 N). Its crystal packing, intermolecular interaction and ESP play an important role in reducing sensitivity. Further, its thermal decomposition temperature is 172.6 °C. This work provides the inspiration for designing nitrogen rich energetic compounds, especially triazene bridges.

INTRODUCTION

Nitrogen-rich compounds are the most promising candidates for energetic compounds because they are environmentally friendly and high-exothermic, high-energy and low-signal.¹⁻⁶ In recent years, nitrogen-rich heterocyclic energetic compounds containing bridging structures have received much attention in the military and aerospace fields. Bridging is regarded as an excellent strategy to combine

high formation heats and high energy to obtain better performance. Among many bridged structures, nitrogen bridged structures are the most desirable, which are different from carbon bridged and oxygen bridged (-CH₂-CH₂-, -CH=CH-, -O-), because their energy does not come from the conventional intramolecular or intermolecular redox reactions of oxygen atoms, but rather from the higher bond energy of the -HN-NH-, -N=N- bonds.⁷⁻⁹ A typical nitrogen bridging structure is listed, the azo (-N=N-) is one of the most efficient bridging structures currently available. Azo-bridged energetic compounds generally have high formation heats and detonation properties, such as the well-known DAAzF (**1**) and TATT (**5**),^{10,11} especially TATT has the highest heats of formation among the reported energetic compounds. Therefore, people are striving to explore new energetic compounds for nitrogen bridging.

The triazene bridges (-N=N-NH-) have a longer chain of nitrogen atoms than the widely studied azo-bridges. A longer catenated nitrogen atom chain represents that the energetic compounds will have higher heats of formation, which is helpful to increase detonation performance. At the same time, the -NH- of triazene bridges can form hydrogen bonding interaction with electron-absorbing groups, which can reduce the sensitivity of energetic compounds. However, it is very difficult to synthesize long nitrogen atom bridges, and this difficulty from their high heat absorption and thermodynamic instability. Therefore, triazene bridges are not common in energetic compounds. The most typical compound with a triazene bridge is 1,1'-(triaz-1-ene-1,3-diyl)bis(1*H*-tetrazol-5-amine) (**2**),¹² which has a continuous N11 in its molecular structure. Its theoretical detonation velocity is 7220 m s⁻¹, and the mechanical sensitivity is lower than that of RDX. However, the neutral compound cannot be obtained in isolation because it is unstable. Mel'nikova reported a triazene bridges compound, 4,4'-(triaz-1-ene-1,3-diyl)bis(3-nitro-1,2,5-oxadiazole) (**4**),¹³ but its detonation properties and stability were not reported. In 2009, Klapötke's group synthesized a high-energy nitrogen-rich compound, bis(methyltetrazolyl)triazenes (**6**), with a triazene bridge from 1-methyl-3-aminotetrazolium by a diazo-N-coupling reaction.¹⁴ The compound shows high detonation properties ($\rho = 1.532 \text{ g cm}^{-3}$ $D = 7982 \text{ m s}^{-1}$), and impact sensitivity (IS = 2.5 J). In 2021, 5,5'-(triaz-1-ene-1,3-diyl)bis(2-methyl-4-nitro-2*H*-1,2,3-triazole) (**3**) was synthesized,¹⁵ which is an excellent insensitive energetic compound (IS>50J, FS=216N), as well as possessing good detonation performance ($D=7720 \text{ m/s}$). Jiang reported 5,5'-dinitro-3,3'-triazene-1,2,4-triazole (**7**) and their ionic compounds that all exhibit excellent detonation properties and mechanical insensitivity.¹⁶ Given these studies, triazene bridges are important for the exploration of novel nitrogen-rich heterocyclic energetic compounds as a rare and excellent bridging structure.

Furazan is one of the most interesting nitrogen-rich structures in the field of energetic compounds, it consists of a five-membered ring composed of C,N,O. It has different characteristics from imidazole, pyrazole, triazole and tetrazole due to the oxygen atoms. It exhibits higher density more excellent oxygen balance and high formation heats, which has led to the birth of many excellent energetic compounds. The

nitrogen rich high-energy compounds of furazan and triazene bridges have been synthesized by Sheremetev, but its performance has not been studied.¹⁷ In this work, 4,4'-(triaz-1-en-1,3-diyl)bis(1,2,5-oxadiazol-3-amine) (**8**) was synthesized using a new route and its structure was characterized. Its detonation properties, thermal stability and mechanical sensitivity were investigated. These compounds show important physical and chemical properties, which give inspiration to the exploration of energetic compounds.

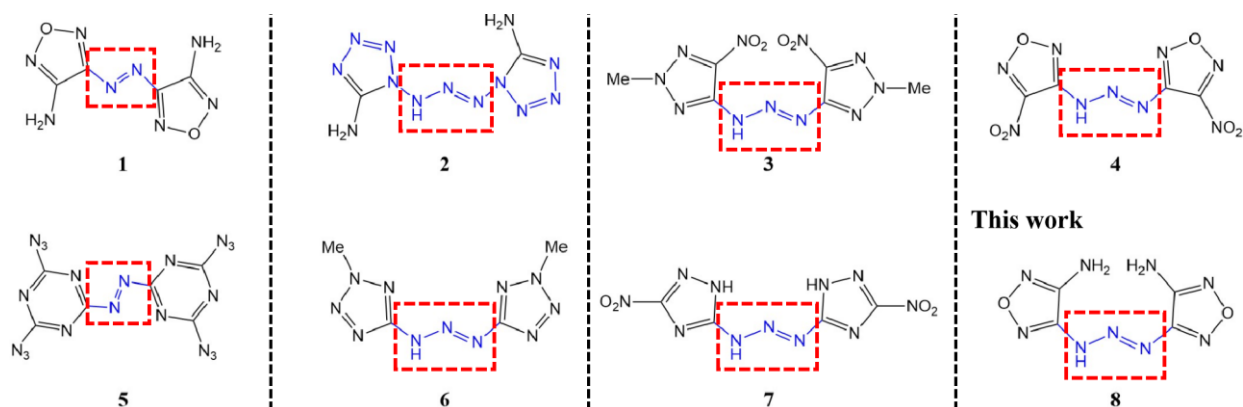
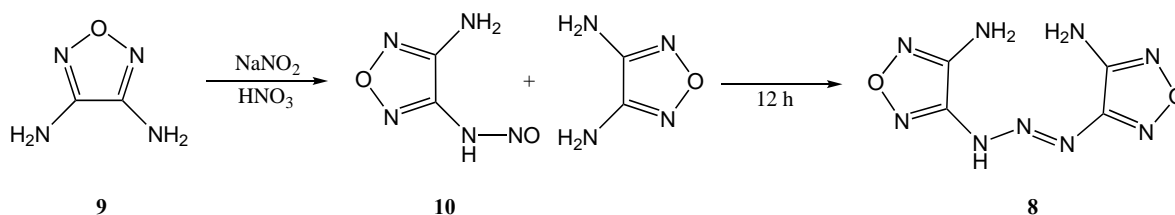


Figure 1. Nitrogen-rich energy-containing compounds linked by azo and triazene bridges

RESULTS AND DISCUSSION

SYNTHESIS

The synthetic route of compound **8** was divided into two steps. First, a portion of 3,4-diaminofurazan (**9**) was diazotized with sodium nitrite in aqueous HNO₃ solution to give **10**. Unreacted **9** and **10** in solution are dehydrated and bridged to give **8**.



Scheme 1. Synthesis route for **8**

SINGLE CRYSTAL STRUCTURE ANALYSIS

Crystals of compound **8** were obtained by slow evaporation of the ethanol solution at room temperature. Single crystal X-ray structure analysis as in Figures 2 and 3. Figure 2a shows the molecular structure of compound **8**. It is evident from the molecular structure and Figure 2b that the molecular structure is nonplanar. The furazan near the NH side has a smaller dihedral angle with the triazene bridge (4.0°),

while the furazan on the other side has a larger dihedral angle with the triazene bridge (19.3°) and the dihedral angle between the two furazan planes is larger (30.7°) with multiple torsions of the longer triazene bridge. In Figure 2c, the molecule crystallizes in the monoclinic system. It belongs to the P 21/n space group with four molecules per cell and has a crystal density of 1.681 g/cm³ at 273 K (1.675 g cm⁻³ at 298 K). Figure 3 shows the compound **8** packing at different angles, and the molecular layer spacing of **8** is 3.34 Å which belongs to Π stacking.¹⁸ Combined with Figure. 3a, b and c, it can be seen that a hydrogen bonding was formed among molecules and molecular layers, which may drastically reduce the sensitivity of the compound.

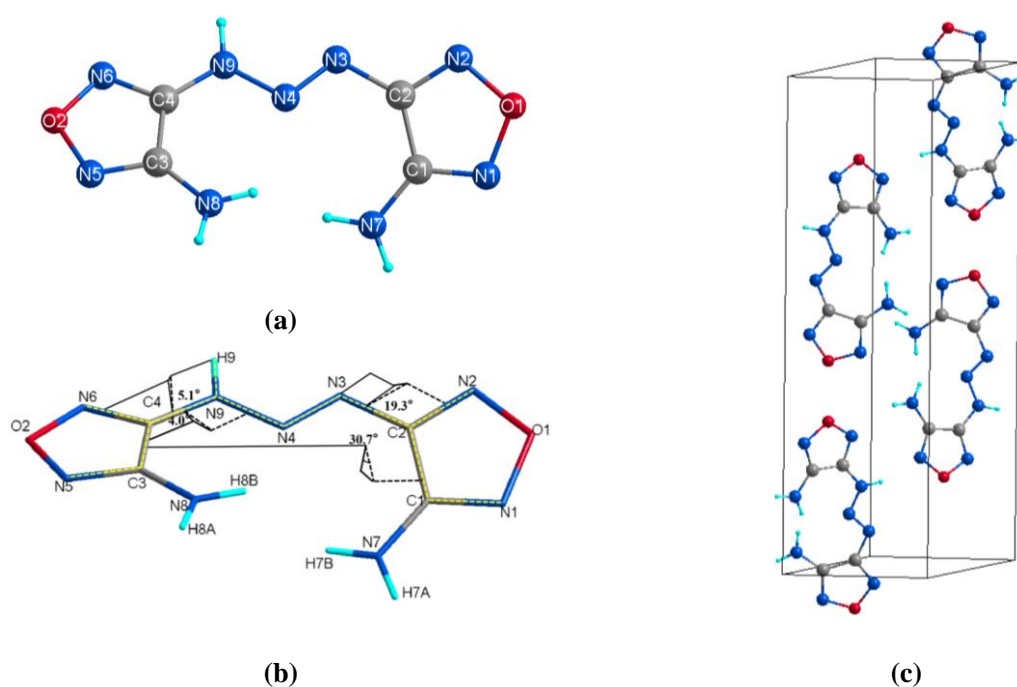


Figure 2. X-Ray structures (single crystal) of **8(a)**. Torsion angle of **8(b)**. A cell of **8(c)**

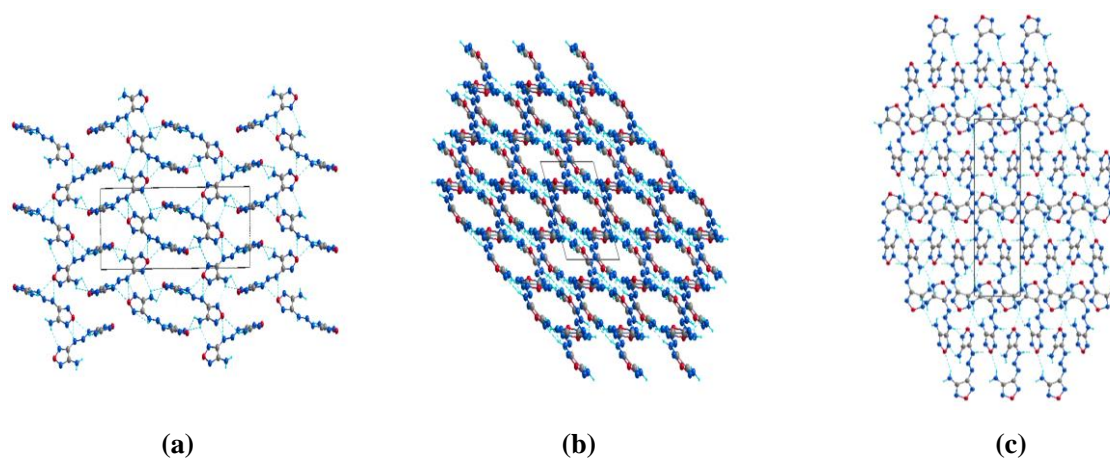


Figure 3. **8** Molecular stacking at different angles

Table 1. Crystal data and structure refinement for crystals

4,4'-(triaz-1-ene-1,3-diyl)bis(1,2,5-oxadiazol-3-amine) (8)			
Moiety formula	C ₄ H ₅ N ₉ O ₂	γ [°]	90
Formula weight	211.17	V [Å ³]	834.18(14)
T[K]	273	Z	4
ρ . [g cm ⁻³]	1.681	μ [mm ⁻¹]	1.212
Crystal description	Monoclinic system	F000	432.0
Space group	P 21/n	h, k, lmax	7, 25, 8
a [Å]	6.1615(6)	Tmin, Tmax	0.865, 0.908
b [Å]	21.2629(19)	θ (max)	66.782
c [Å]	7.0630(6)	R	0.0802(1178)
α [°]	90	wR2	0.2083(1484)
β [°]	115.645	CCDC number	2290524

PHYSICOCHEMICAL PROPERTIES

Detonation velocity and pressure are important properties that reflect the energy level of energetic compounds. Thus, they have received great attention. After synthesizing **8**, its detonation properties and performance have been investigated. The heats of formation (ΔH_f) of **8** was calculated to be about 926.32 kJ mol⁻¹ by Gaussian 09 (Revision D.01), isobonding reaction combined and atomization method,¹⁹⁻²¹ which shows the high heats of formation. The detonation velocity (D) and pressure (P) of **8** were evaluated by the K-J formula using the crystal density and the calculated heat of formation.²² The results show that the detonation velocity and pressure of **8** are 8151 m s⁻¹ and 28.55 GPa, which are better than TNT (D=6881 m s⁻¹ P=22.80 GPa) and DAAzF (D=7592 m s⁻¹ P=24.94 GPa), and are close to the energy level of RDX (D=8560 m/s P=34.55 GPa).

The safety properties of energetic compounds are great important in their production, storage and use. The standard safety properties include thermal stability and mechanical sensitivity. Thermogravimetric-differential thermal analysis (TG-DTA) was taken to analyze the thermal stability properties of **8**. Compound **8** was tested in a nitrogen atmosphere at a heating rate of 5 °C min⁻¹. There was only one peak of **8** on the DTA curve with a peak value of 172.6 °C. The TG curve showed that **8** decomposed rapidly near 172.6 °C with a weight loss of 88.9%. The results indicate that the thermal decomposition temperature of **8** is low than that of the similar structure DAAzF, which may be caused by the fast break of the triazole bridge under thermal action. To verify this supposition, we use bond dissociation enthalpies (BDEs) as a measure of thermal decomposition.²³ The calculations showed that

the BDEs of the triazene bridges N-NH in compound **8** are about 138.5 kJ mol⁻¹, which is lower than that of DAAzF (azo and furazan N-C, 206.2 kJ mol⁻¹), which is in agreement with the experiment.

Table 2. Physicochemical properties of **8**, DAAzF, RDX and TNT

	8	DAAzF	RDX	TNT
Formula	C ₄ H ₅ N ₉ O ₂	C ₄ H ₄ N ₈ O ₂	C ₃ H ₆ N ₆ O ₆	C ₇ H ₅ N ₃ O ₆
Molecular mass [g/mol]	211	196	222	227
ρ ^a [g cm ⁻³]	1.68	1.72	1.81	1.64
Ω ^b [%]	-64.45	-65.31	-21.62	-74.01
IS ^c (J)	40	>60	7	15
FS ^d (N)	289	>360	120	>353
T _{dec} ^e [°C]	172.6	327	210	295
V _{det.} ^f [m s ⁻¹]	8151	7592	8560	6881
P ^g [GPa]	28.55	24.94	34.55	22.80
ΔH _{fm} [kJ mol ⁻¹]	926.32 ^h	536 ⁱ	86.3	-63.0
E _{BDE} [kJ mol ⁻¹]	138.5 ^j	206.2 ^k	-	-
N+O/%	74.9	73.5	81.1	60.8

^aDensity (measured with a gas pycnometer at 298 K), ^bOxygen balance based on CO₂ for C H N O_{abcd}: OB (%) = 16×(d-2×a-1/2×b)/Mw, ^cImpact sensitivity evaluated by a standard BAM fall-hammer, ^dFriction sensitivity evaluated by a BAM friction tester, ^eDecomposition temperature, ^fDetonation velocity, ^gDetonation pressure, ^hCalculated heat of formation, ⁱData from the literature, ^jCalculated Bond Dissociation Energy of **8** and DAAzF.

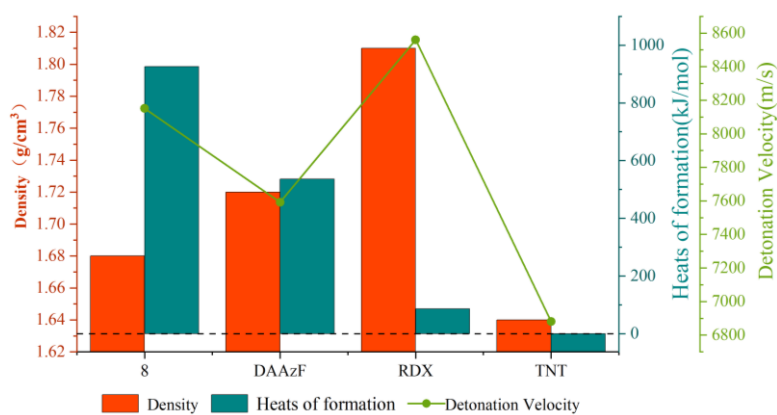


Figure 4. Comparison of density, enthalpy of production, and detonation velocity of **8**, DAAzF, RDX and TNT

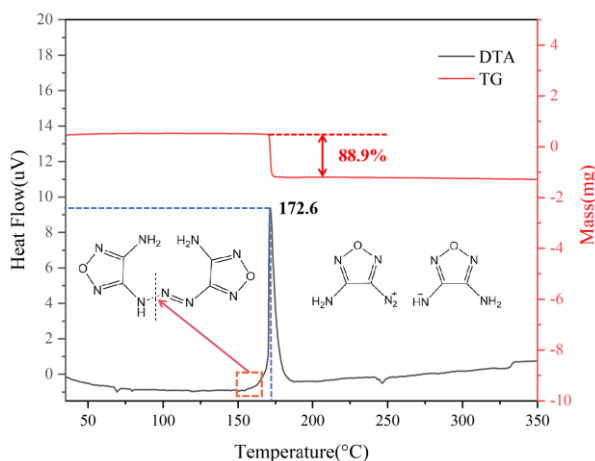


Figure 5. TG-DTA curves for **8**

The mechanical sensitivity of compound **8** was evaluated by BAM-type impact and friction tester. Its impact sensitivity and friction sensitivity are 40 J and 289 N. These results show that compound **8** has very excellent insensitivity, which is superior to TNT, RDX. For this, we find the reason to explain it rationally.

There is usually a relationship between surface electrostatic potential (ESP) and sensitivity in energetic materials. According to previous studies, the higher positive ESP value and area leads to compounds having higher sensitivity.²⁴ For this reason, their ESP was visualized by VMD.^{25,26} In Figure 6, the positive charge of the hydrogen atom in compound **8** causes the amine groups and triazine bridges to show a positive ESP (red region), and the furazan rings shows negative ESP (blue region). The bars show the area of different electrostatic strengths, the ESP of compound **8** being larger in the negative and low positive areas, while smaller in the high positive areas. Thus compound **8** has a lower sensitivity. This is

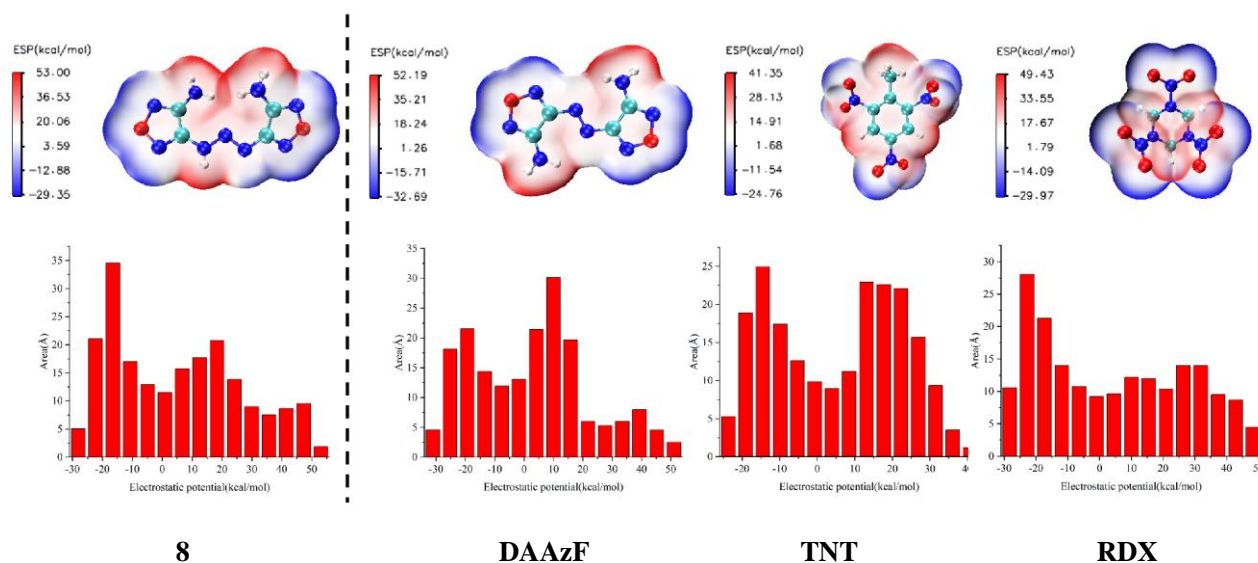


Figure 6. Surface electrostatic potential of **8**, DAAzF, TNT and RDX

similar to DAAzF. TNT and RDX have larger areas at higher positively charged values than compound **8** and DAAzF, which is why they are more sensitive than compound **8**.

Previous studies have shown that hydrogen bonding in energetic compounds mitigates internal strains due to impact and friction, thus making energetic compounds insensitive.²⁷ IRI, Hirschfeld surfaces, and 2D fingerprinting are useful as a tool that can quickly show the hydrogen bonding regions of compounds, as well as the intermolecular hydrogen bonding (H...O O...H and H...N N...H) percentage, which is very important for the study of the stability of energetic compounds.^{28,29} Therefore, we investigated the hydrogen bonding of compound **8** by IRI, Hirschfeld surface and 2D fingerprinting. The IRI data in Figure 7a and b, they show that there is no intramolecular hydrogen bonding interaction for **8**, only van

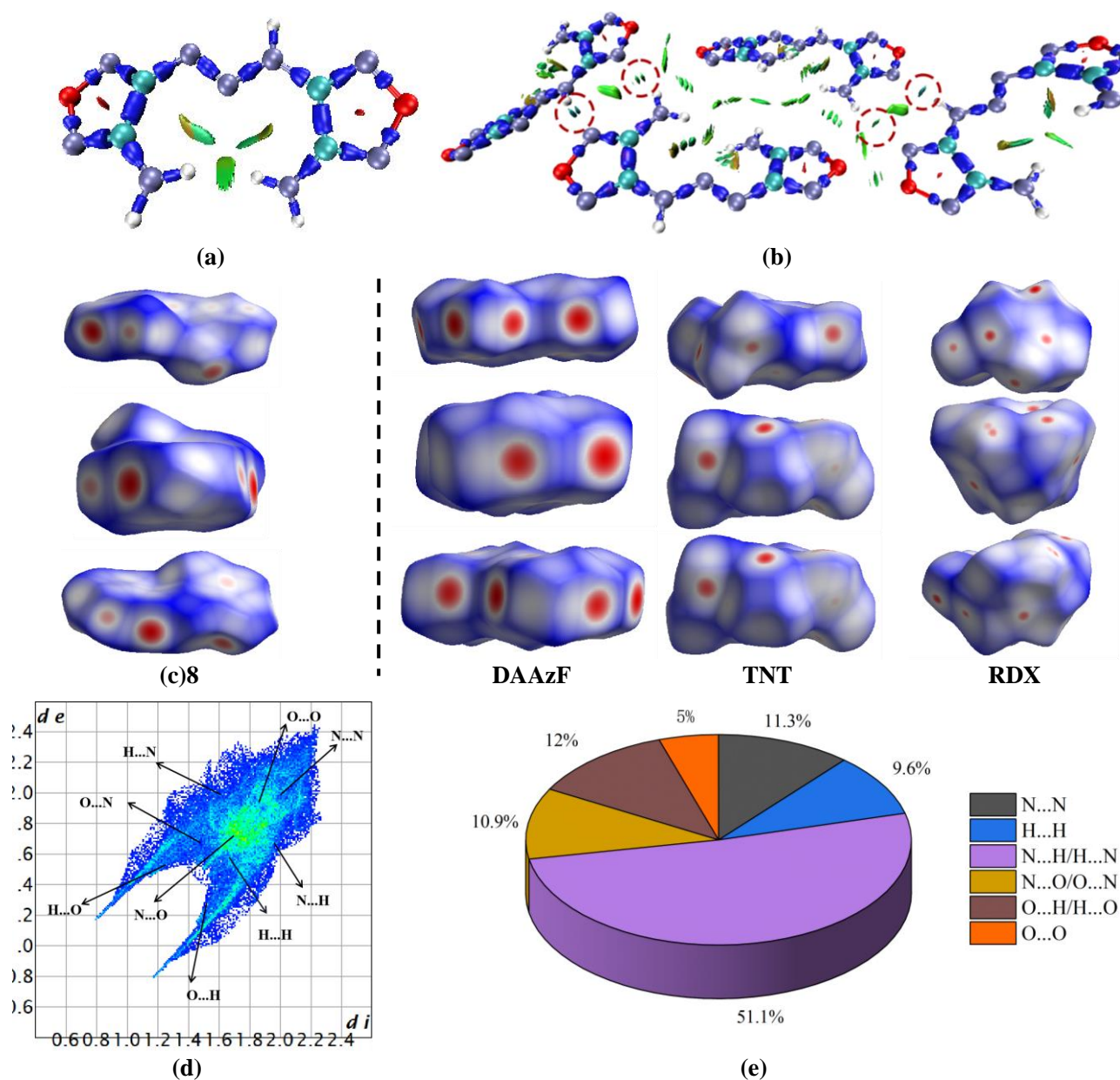


Figure 7. IRI, Hirschfeld surfaces and 2D fingerprint maps of **8**

der Waals forces and intermolecular hydrogen bonding. Figure 8c shows the Hirshfeld surface at different angles, some red dots represent intermolecular hydrogen bonding or weak hydrogen bonding of **8**. They are mainly distributed around the amino group, the triazole bridge, and the oxygen atom of the furazan. These weakly interacting populations can also be obtained directly from the 2D fingerprinting. Combined with Figure 7d and 7e, it can be seen that the intermolecular hydrogen bonding of **8** (H...O O...H and H...N N...H) neighborhood's accounted for 63.1% of the weak interactions, which is better than TNT (44%), RDX (59.1%), and DAAzF (61.7%). The higher hydrogen bonding occupancy reduces the free space in the crystal structure to reduce the generation of localized hot spots due to impact and friction.

In addition to hydrogen bonding, the type of crystal packing is also an important factor affecting sensitivity. For example, DAAzF, its molecular packing type, is planar layered packing. When receiving external impacts and friction, it allows interlayer sliding to avoid the generation of hot spots, which reduces the sensitivity, as does the wavelike layered packing.²⁷ These two stacking modes facilitate the desensitization of energetic compounds. Therefore, we investigated the stacking type of **8**. In Figure 8, **8** possesses a wavelike layered packing with a small angle. This will allow the molecular layer of **8** to slide better to obtain low sensitivity.

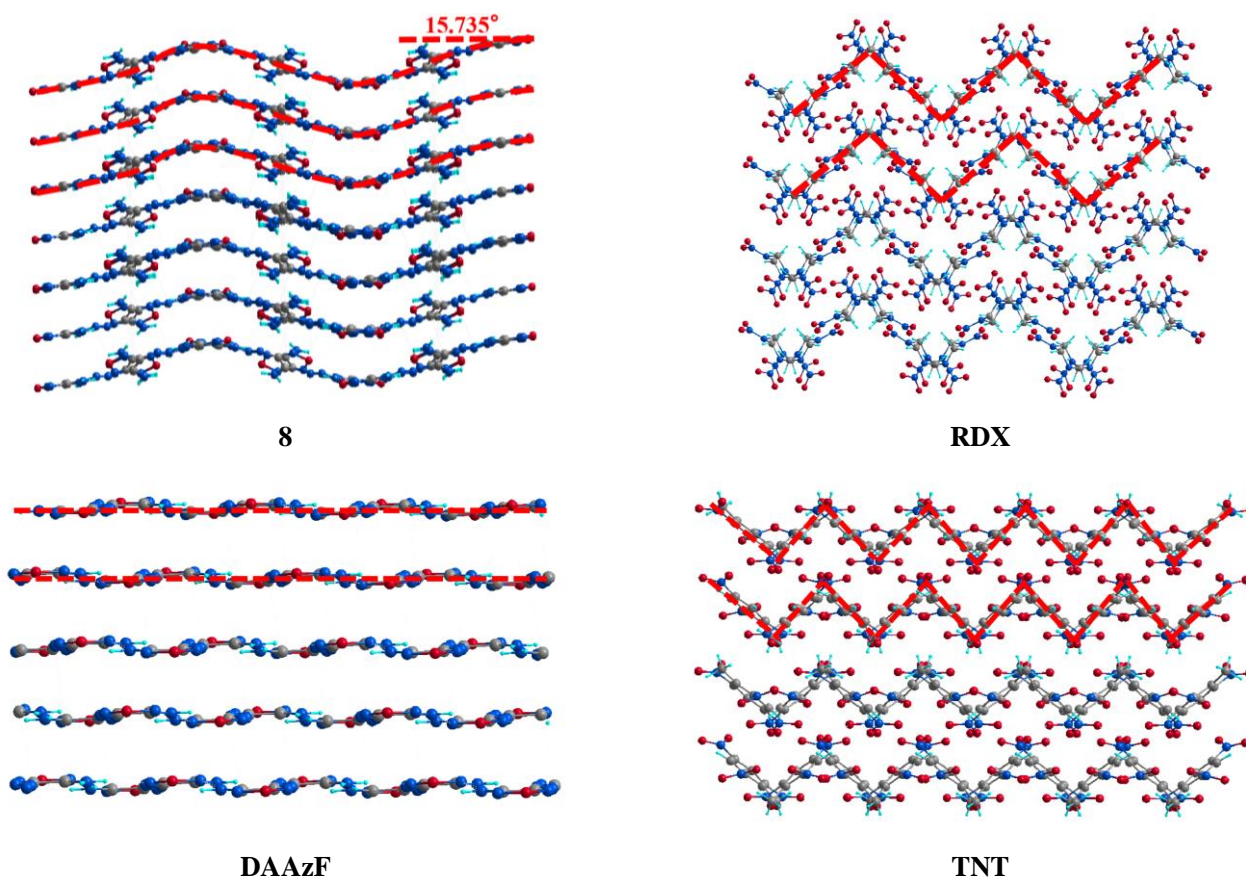


Figure 8. Type of molecular layer stacking for **8**, DAAzF, RDX and TNT

CONCLUSIONS

In summary, 4,4'-(triaz-1-ene-1,3-diyl)bis(1,2,5-oxadiazol-3-amine) was synthesized and characterized by elemental analyses, IR, NMR, and single-crystal X-ray diffraction. A study of the molecular structure and physicochemical properties of 4,4'-(triaz-1-ene-1,3-diyl)bis(1,2,5-oxadiazol-3-amine) reveals that this compound exhibits particularly high formation heats ($\Delta H_f=926.32 \text{ kJ mol}^{-1}$) which is higher than that of all currently reported furazan-based energetic compounds, excellent detonation performance ($D=8151 \text{ m s}^{-1}$, $P=28.55 \text{ GPa}$). In addition, this compound is insensitive to external mechanical stimuli ($IS=40 \text{ J FS}=289 \text{ N}$). Its crystal packing, intermolecular interaction and ESP play an important role in reducing sensitivity. Further, its thermal decomposition temperature is $172.6 \text{ }^\circ\text{C}$. Good performance not only highlights 4,4'-(triaz-1-ene-1,3-diyl)bis(1,2,5-oxadiazol-3-amine) as an excellent energetic compound, but also shows that the pairing of triazene bridges and furazans is a good choice for building energetic compounds.

EXPERIMENTAL

Caution: Although we have not experienced any difficulties in preparing and handling these new energetic materials, proper protective precautions must be used. All compounds should be handled with care using the best safety practices.

4,4'-(Triaz-1-ene-1,3-diyl)bis(1,2,5-oxadiazol-3-amine) (8) At low temperature ($0 \text{ }^\circ\text{C}$) with stirring, 5 mL of distilled water was poured into a 25 mL three-necked flask and 3,4-diaminofurazan (0.1 g, 0.001 mol) was added to form a suspension. Nitric acid solution of sodium nitrite (NaNO_2 0.42 g, 0.00061 mol; 98% nitric acid 0.5 mL; water 2 mL) was prepared and slowly added to the reaction mixture. The temperature was then raised to $25 \text{ }^\circ\text{C}$ and the reaction was kept this temperature for 12 h. At the end of the reaction, yellow particles were obtained by filtration in 81.3% yield. **IR** cm^{-3} : 3462, 3350, 2872, 1638, 1598, 1561, 1494, 1440, 1415, 1337, 1231, 1121, 1001, 932, 873, 743, 669, 607. **^1H NMR**(500MHz, $\text{DMSO-}d_6$, $25 \text{ }^\circ\text{C}$, ppm) δ : 6.81, 13.85-14.57. **^{13}C NMR**(150MHz, $\text{DMSO-}d_6$, $25 \text{ }^\circ\text{C}$, ppm): 150.76, 151.12.

Elemental analysis for $\text{C}_4\text{H}_5\text{N}_9\text{O}_2$, Anal. Calcd (%): C 22.75, H 2.39, N 59.70. Found(%): C 22.73, H 2.29, N 59.58.

REFERENCES AND NOTES

1. J. M. Veauthier, D. E. Chavez, B. C. Tappan, and D. A. Parrish, *J. Energ. Mater.*, 2010, **28**, 229.
2. J. Zhang and J. M. Shreeve, *J. Am. Chem. Soc.*, 2014, **136**, 4437.
3. P. F. Pagoria, M. X. Zhang, N. B. Zuckerman, A. J. DeHope, and D. A. Parrish, *Chem. Heterocycl. Compd.*, 2017, **53**, 760.

4. L. L. Fershtat and N. N. Makhova, *ChemPlusChem*, 2020, **85**, 13.
5. J. Zhang, Z. Wang, Y. Hsieh, B. Wang, H. Huang, J. Yang, and J. Zhang, *RSC Adv.*, 2020, **10**, 2519.
6. P. Yin and J. M. Shreeve, *Adv. Heterocycl. Chem.*, 2017, **121**, 89.
7. Y. Qu and S. P. Babailov, *J. Mater. Chem. A*, 2018, **6**, 1915.
8. J. R. Yount, M. Zeller, and E. F. C. Byrd, *J. Mater. Chem. A*, 2020, **8**, 19337.
9. Y. Tang, C. He, H. Gao, and J. M. Shreeve, *J. Mater. Chem.*, 2015, **3**, 15576.
10. A. Gunasekaran, T. Jayachandran, and J. H. Boyer, *J. Heterocycl. Chem.*, 1995, **32**, 1405.
11. M. H. V. Huynh and M. A. Hiskey, *Angew. Chem. Int. Ed.*, 2004, **43**, 4924.
12. Y. Tang, H. Yang, B. Wu, X. Ju, C. Lu, and G. Cheng, *Angew. Chem. Int. Ed.*, 2013, **52**, 4875.
13. T. M. Mel'nikova, T. S. Novikova, L. I. Khmel'nitskii, and Aleksei B. Sheremetev, *Mendeleev Commun.*, 2001, **11**, 30.
14. T. M. Klapötke, N. K. Minar, and J. Stierstorfer, *Polyhedron*, 2009, **28**, 13.
15. S. B. Feng, F. S. Li, X. Y. Zhao, Y. D. Qian, T. Fei, P. Yin, and S. P. Pang, *Energ. Mater. Front.*, 2021, **2**, 125.
16. X. Jiang, Y. Yang, H. Du, B. Yang, P. Tang, B. Wu, and C. Ma, *Dalton Trans.*, 2023, **52**, 5226.
17. A. B. Sheremetev, V. G. Andrianov, E. V. Mantseva, E. V. Shatunova, N. S. Aleksandrova, I. L. Yudin, D. E. Dmitriev, B. B. Averkiev, and M. Yu. Antipin, *Russ. Chem. Bull.*, 2004, **53**, 596.
18. C. A. Hunter and J. K. Sanders, *J. Am. Chem. Soc.*, 1990, **112**, 5525.
19. T. Fei, Y. Du, and S. Pang, *RSC Adv.*, 2018, **8**, 10215.
20. E. Byrd and B. M. Rice, *J. Phys. Chem. A*, 2009, **113**, 5813.
21. P. Politzer, S. Jane, and J. Murray, *J. Mol. Struct. : THEOCHEM.*, 2001, **573**, 1.
22. M. J. Kamlet and S. J. Jacobs, *JCP*, 1968, **4**, 23.
23. S. J. Blanksby and E. G. Barney, *Acc. Chem. Res.*, 2003, **36**, 255.
24. D. Mathieu, *Ind. Eng. Chem. Res.*, 2017, **56**, 8191.
25. T. Lu and F. Chen, *J. Comput. Chem.*, 2012, **33**, 580.
26. H. W. Dalke and K. A. Schulten, *J. Mol. Graph. Model.*, 1996, **14**, 33.
27. W. J. Geng, Q. Ma, Y. Chen, W. Yang, Y. F. Jia, J. S. Li, Z. Q. Zhang, G. J. Fan, and S. M. Wang, *Cryst. Growth Des.*, 2020, **20**, 2106.
28. T. Lu and Q. Chen, *Chemistry - Methods*, 2021, **1**, 231.
29. S. K. Wolff, D. J. Grimwood, J. J. McKinnon, M. J. Turner, D. Jayatilaka, and M. A. Spackman, M.A. (2012) Crystal Explorer 3.0. University of Western Australia, Pert.